

MADD-4/Punctin and Neurexin Organize *C. elegans* GABAergic Postsynapses through Neuroligin

Highlights

- *C. elegans* neuroligin specifically localizes to GABA postsynapses
- GABA_A receptors fail to cluster at postsynaptic sites in the absence of neuroligin
- Neurexin and Punctin/MADD-4 redundantly control GABA_AR clustering
- Punctin/MADD-4 binds to neuroligin and to neurexin

Authors

Géraldine S. Maro, Shangbang Gao, Agnieszka M. Olechwier, ..., Engin Özkan, Mei Zhen, Kang Shen

Correspondence

zhen@lunenfeld.ca (M.Z.), kangshen@stanford.edu (K.S.)

In Brief

Maro et al. show that the ADAMTS-like molecule Punctin/MADD-4 can bind the neuronal cell adhesion molecules neuroligin and neurexin. Using *C. elegans* as a model system, they show that Punctin/MADD-4, neurexin, and neuroligin control the clustering of postsynaptic GABA receptors.



MADD-4/Punctin and Neurexin Organize *C. elegans* GABAergic Postsynapses through Neuroligin

Géraldine S. Maro,^{1,4} Shangbang Gao,^{2,4} Agnieszka M. Olechwiec,³ Wesley L. Hung,² Michael Liu,¹ Engin Özkan,³ Mei Zhen,^{2,*} and Kang Shen^{1,*}

¹Howard Hughes Medical Institute, Department of Biology, Stanford University, Stanford, CA 94305, USA

²Lunenfeld-Tanenbaum Research Institute, Mount Sinai Hospital, Toronto, ON M5G1X5, Canada

³Department of Biochemistry and Molecular Biology, University of Chicago, Chicago, IL 60637, USA

⁴Co-first author

*Correspondence: zhen@lunenfeld.ca (M.Z.), kangshen@stanford.edu (K.S.)

<http://dx.doi.org/10.1016/j.neuron.2015.05.015>

SUMMARY

At synapses, the presynaptic release machinery is precisely juxtaposed to the postsynaptic neurotransmitter receptors. We studied the molecular mechanisms underlying this exquisite alignment at the *C. elegans* inhibitory synapses. We found that the sole *C. elegans* neuroligin homolog, NLG-1, localizes specifically at GABAergic postsynapses and is required for clustering the GABA_A receptor UNC-49. Two presynaptic factors, Punctin/MADD-4, an ADAMTS-like extracellular protein, and neurexin/NRX-1, act partially redundantly to recruit NLG-1 to synapses. In the absence of both MADD-4 and NRX-1, NLG-1 and GABA_A receptors fail to cluster, and GABAergic synaptic transmission is severely compromised. Biochemically, we detect an interaction between MADD-4 and NLG-1, as well as between MADD-4 and NRX-1. Interestingly, the presence of NRX-1 potentiates binding between Punctin/MADD-4 and NLG-1, suggestive of a tripartite receptor ligand complex. We propose that presynaptic terminals induce postsynaptic receptor clustering through the action of both secreted ECM proteins and *trans*-synaptic adhesion complexes.

INTRODUCTION

Precise apposition between the presynaptic release machinery and postsynaptic receptors ensures that neurotransmitters trigger rapid and reliable synaptic response. Several mechanisms contribute to the precise alignment of synaptic membranes. At the vertebrate neuromuscular junction (NMJ), motor axon-secreted agrin plays a critical role in synapse maturation by clustering postsynaptic acetylcholine receptors (Sanes and Lichtman, 1999). Direct interaction between calcium channels and synaptic laminin helps to precisely localize active zones at the NMJ (Nishimune et al., 2004). In the central nervous system,

many “synaptic organizers” have been described. These organizers include *trans*-synaptic adhesion molecules like neurexin and neuroligin, secreted synaptic adaptor proteins (Cbln), as well as glia-derived factors like thrombospondin (Siddiqui and Craig, 2011). The synaptogenic activity of these molecules was typically studied in excitatory glutamatergic synapses *in vitro*.

Among the synaptic adhesion molecules, the best-studied neurexin and neuroligin pair plays important roles in the maturation and function of synapses (Südhof, 2008). Neuroligin and neurexin bind to each other and are sufficient to induce pre- and postsynaptic differentiation, respectively, *in vitro* (Ichtchenko et al., 1995; Dean et al., 2003; Graf et al., 2004). Despite this well-established synaptogenic activity, neuroligin and neurexin do not seem to be required for synapse development in vertebrates (Varoqueaux et al., 2006), but might be in other organisms, as suggested by studies in *Drosophila* (Li et al., 2007). Two of the four rodent neuroligins, NLGN1 and NLGN2, show preferential association with excitatory and inhibitory postsynapses, respectively (Song et al., 1999; Varoqueaux et al., 2004). Importantly, the genetic relationship between each of the neuroligins and neurexins is not established in vertebrates due to high level of redundancy in each gene family. It is therefore not known whether neuroligins’ postsynaptic localization requires the function of neurexins. Indeed, in *Drosophila*, while loss of neurexin (*dNrx*) or neuroligin (*dNlg1*) causes similar synaptic defects, *dNrx* binding is not absolutely required for *dNlg1* function (Banovic et al., 2010). The *C. elegans* genome encodes a single neuroligin ortholog, NLG-1, and a single neurexin ortholog, NRX-1. Previous studies have shown that the *C. elegans* *nlg-1* mutant displays sensory processing defects and an impairment in retrograde signaling at the cholinergic NMJs.

We took advantage of the relative simplicity of *C. elegans* to investigate the role of neuroligin at postsynaptic sites. We found that NLG-1 specifically localizes to GABAergic postsynaptic NMJs. Consistent with this localization, *nlg-1* null mutants display reduced GABA_A receptor (GABA_AR) clustering and a reduction in spontaneous inhibitory current (mIPSC) frequency and amplitude. Both defects were rescued by restoring NLG-1 expression in body wall muscles. Our results also indicate that NLG-1 relies on extracellular interactions for GABA_AR clustering and that its binding partner NRX-1 is dispensable for such a

function. However, we find that in the absence of NRX-1 and Punctin/MADD-4, NLG-1 and GABA_AR clustering is severely compromised.

RESULTS

Neuroigin Clusters GABA_A Receptors at Postsynaptic Sites

The *C. elegans* body wall muscles, which express NLG-1 (Hunter et al., 2010), receive direct synaptic inputs from both cholinergic and GABAergic motor neurons. To determine the subcellular localization of NLG-1 in muscles, we expressed a functional NLG-1::YFP (Hunter et al., 2010) using a muscle-specific promoter and observed discrete puncta along the nerve cords (Figure 1A), reminiscent of a postsynaptic distribution at NMJs. Colocalization analyses with GABAergic and cholinergic presynaptic markers revealed that NLG-1::YFP is precisely apposed to inhibitory presynaptic terminals and is excluded from excitatory cholinergic synapses (Figures 1A–1C), similar to the specific NLGN2 localization at GABAergic postsynaptic terminals in mammals (Varoqueaux et al., 2004).

The specific localization of muscle NLG-1 at inhibitory postsynaptic sites raises the possibility that it might play a role in the assembly and/or function of this synapse. The heteromultimeric GABA_AR is composed of subunits encoded by the *unc-49* locus in *C. elegans* (Richmond and Jorgensen, 1999; Bamber et al., 1999). Therefore, we analyzed the distribution of the GABA_A UNC-49 receptor in the absence of NLG-1. A fluorophore-tagged UNC-49B::YFP fusion protein forms clusters that appose the GABAergic presynaptic sites, labeled with SNB-1::CFP, similar to the antibody-labeled UNC-49 endogenous receptors (Figure 1E and Gally and Bessereau, 2003). Interestingly, in *nlg-1(ok259)* animals, we observed diffuse YFP fluorescence outlining the muscle cell membranes (Figures 1F and 1H) and failed to detect any obvious UNC-49B::YFP puncta above that diffuse fluorescence component, suggesting that UNC-49B::YFP properly reaches the plasma membrane but fails to cluster in the absence of NLG-1. SNB-1::CFP puncta were still visible on the presynaptic side (Figure 1F). We asked whether GABA_ARs were reciprocally required for NLG-1 localization by examining NLG-1::YFP expression in the *unc-49(e382)* mutant background. The distribution of NLG-1::YFP clusters was not affected by the lack of UNC-49 (Figure 1D), suggesting that NLG-1 lies upstream of the GABA_AR in the postsynaptic assembly hierarchy, similar to observations made in vertebrate neurons (Patrizi et al., 2008).

Consistent with its postsynaptic localization, expression of NLG-1 or NLG-1::CFP under the control of two different muscle-specific promoters fully rescued the UNC-49B::YFP clustering defects, as did expression of NLG-1 under its endogenous promoter from a genomic fosmid (Figures 1G and 1H). In contrast, expression of NLG-1 in the presynaptic inhibitory neurons did not restore UNC-49B::YFP clustering (Figure 1H). These results suggest that NLG-1 functions cell autonomously in the body wall muscles to form or maintain GABA_AR clusters at the inhibitory postsynapse. They are also consistent with the report that a subset of GABAergic postsynaptic specializations fail to form in the *NLGN2*^{−/−} mutant mouse (Poulopoulos et al., 2009).

neuroigin Mutants Show Defects in GABAergic Synaptic Transmission

To investigate the functional consequence of the defective postsynaptic GABA_AR clustering in *nlg-1(ok259)* mutants, we examined postsynaptic currents in body wall muscles through whole-cell patch-clamp recording. Under our recording conditions, the reversal potentials of cholinergic and GABAergic receptors were +20 mV and −30 mV, respectively (Gao and Zhen, 2011; Figure 2A). When the body wall muscles were held at −30 mV, only inward, spontaneous excitatory mEPSCs were detected (Figure 2B). The identity of these mEPSCs was confirmed by their sensitivity to the application of the ionotropic acetylcholine receptor blocker D-tubocurarine (d-TBC, 0.5 mM) (Figure 2B). When the muscle membrane potential was held at −10 mV, both inward (mEPSCs) and outward (mIPSCs) currents were recorded. The outward currents were insensitive to d-TBC, whereas the inward currents were blocked by d-TBC, confirming that the outward currents specifically represented GABAergic mIPSCs (Figure 2B).

Using this protocol, we found that both the frequency and amplitude of mIPSCs were markedly reduced in *nlg-1(ok259)* mutants, as compared to wild-type animals (Figures 2C–2F). These defects could result from a decreased release probability at presynaptic terminals, or from a reduction of GABA_ARs on the postsynaptic membrane. Because these defects were fully rescued to a wild-type level by expressing NLG-1::CFP specifically in muscles (Figure 2C–2F), and because the presynaptic GABAergic terminals appear normal when examined with synaptic vesicle markers (Figure 1F), we favor the latter explanation. It can be noted that overexpression of NLG-1 did not lead to an increase in mIPSC frequency, suggesting that NLG-1 might not be a rate-limiting factor for the inhibitory miniature currents.

To verify whether NLG-1 is specifically required for the clustering of the GABA_AR or for its insertion on the plasma membrane, we tested the evoked response in muscles upon exogenous GABA (0.5 mM) application. We found no significant difference in the amplitude or kinetics of the evoked GABAergic currents in *nlg-1(ok259)* mutants and wild-type animals, suggesting that functional GABA_ARs are present on muscle cell membranes in *nlg-1* mutant (Figures 2G and 2H).

Together with the visual phenotype observed with the UNC-49::YFP marker, these results strongly argue that NLG-1 is crucial to cluster surface GABA_ARs at postsynaptic sites. Interestingly, a similar reduction in spontaneous inhibitory postsynaptic currents has been described in NL2 knockout mice (Poulopoulos et al., 2009) and more recently in mice models of ASD-associated NL3 mutations (Rothwell et al., 2014).

Consistent with a previous report (Hunter et al., 2010), we did not observe obvious locomotory behavioral phenotype in these animals (data not shown). This finding raises questions about the necessity of GABA signaling for *C. elegans* locomotion. A complete abolishment of GABAergic synaptic transmission (e.g., the *unc-25/GAD* or *unc-49/GABAa* mutants) leads to the “shrinker” phenotype, where animals exhibit hypercontraction, but retain the ability for sinusoidal movements (McIntire et al., 1993). Hence, it is possible that some GABA_AR molecules form clusters that are beyond our detection threshold with the GABA_AR::YFP marker and sufficient to drive normal synaptic function during locomotion.

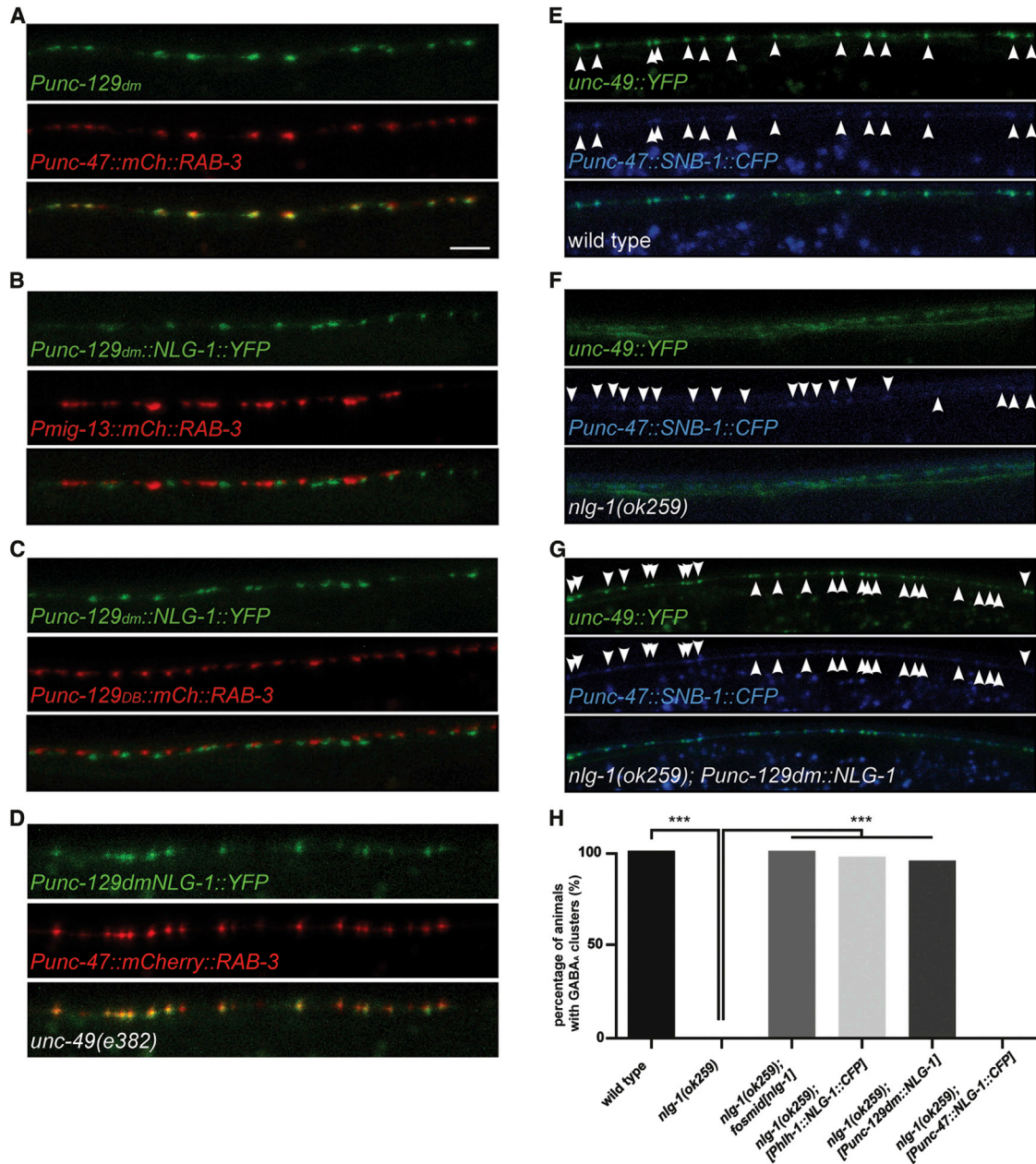


Figure 1. NLG-1 Functions in Muscles to Cluster Synaptic GABA_A Receptors

(A–C) NLG-1::YFP puncta in muscle cells are apposed to GABAergic presynaptic terminals from the D-type motor neuron (A) in the dorsal nerve cord and intercalate with excitatory cholinergic terminals from the A-type (B) or B-type (C) motor neurons. In all panels, NLG-1 is expressed under the control of a fragment of the *unc-129* promoter restricted to dorsal muscle cells, and the presynaptic marker mCherry::RAB-3 is expressed either from the D-type-specific *unc-47* promoter (A), the DA9-specific promoter *mig-13* (B), or the DB-specific promoter *unc-129* (C). Arrowheads point to NLG-1::YFP puncta.

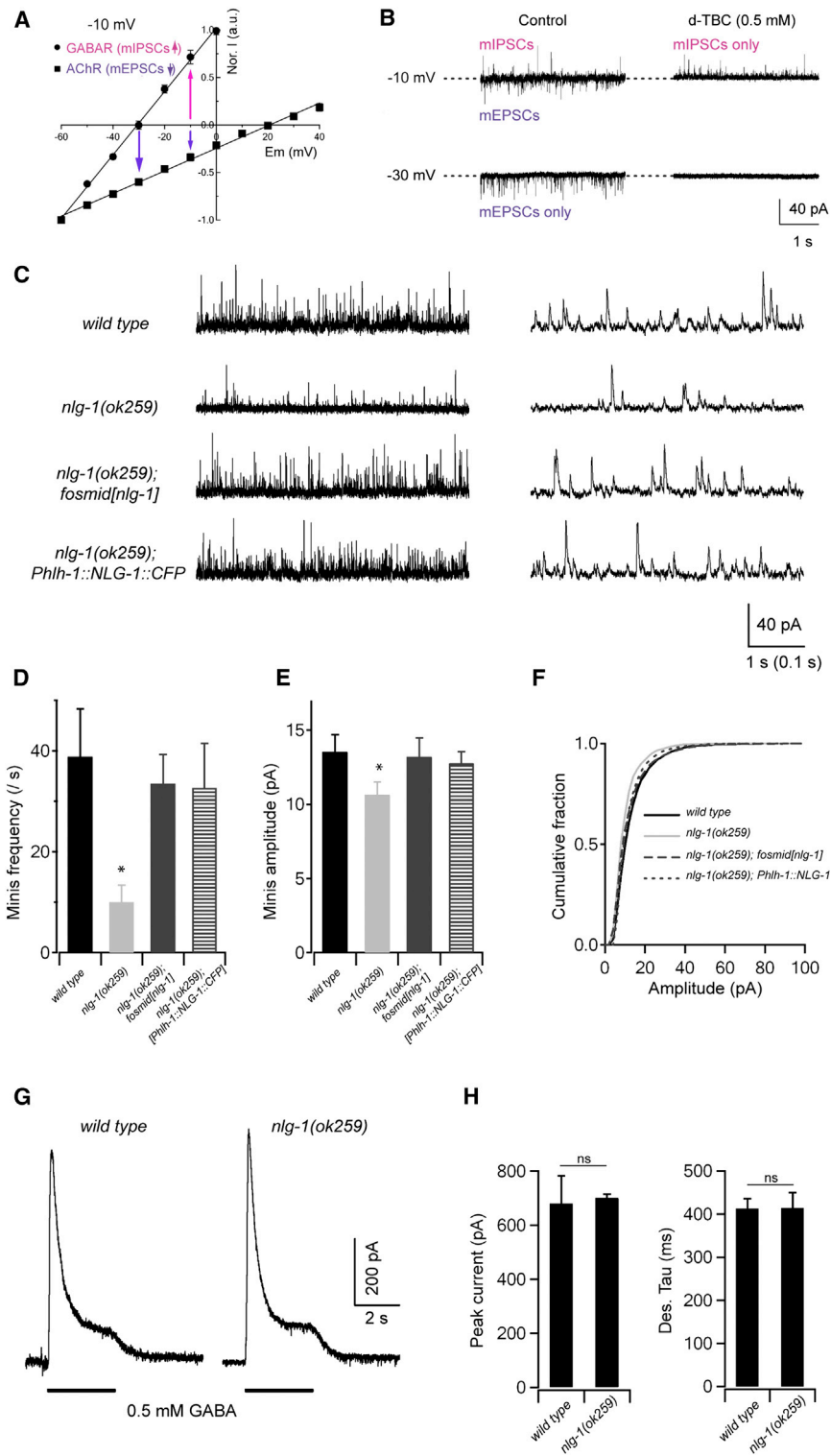
(D) NLG-1::YFP clusters normally in *unc-49(e382)* animals lacking the GABA_AR.

(E) A YFP-tagged UNC-49 GABA_AR (top) forms clusters apposite to GABAergic presynaptic terminals labeled with a SNB-1::CFP marker (middle).

(F) In *nlg-1(ok259)* mutants, UNC-49::YFP is diffuse on the muscle cell plasma membrane (top).

(G) Expression of NLG-1 specifically in muscle cells in *nlg-1(ok259)* animals fully rescues the UNC-49::YFP clustering defect.

(H) Quantification of UNC-49::YFP clustering in wild-type, *nlg-1(ok259)* mutants, and transgenic *nlg-1(ok259)* animals expressing NLG-1 under the control of various promoters. Expression of NLG-1 in muscles is sufficient to restore UNC-49::YFP clustering in *nlg-1(ok259)* mutants. Arrowheads point to SNB-1::CFP puncta. $p < 0.001$, Fisher's exact test. Scale bar: 5 μ m.



NLG-1 Localizes to Inhibitory Synapses Independently of Postsynaptic Scaffold Proteins and of Its Known Ligand NRX-1

Neuroligins are known to interact with a variety of extracellular and intracellular partners, including neurexins, thrombospondin,

Figure 2. NLG-1 Is Required for Normal GABAergic Synaptic Transmission

(A–H) Spontaneous inhibitory currents show reduced amplitude and frequency in *nlg-1* mutants. A protocol for recording GABAergic mIPSCs at the dissected muscle preparation is shown in (A) and (B). In the recording solutions (A), the reversal potentials are around -30 mV and $+20$ mV for muscular GABA_ARs and ACh receptors, respectively (adapted from Gao and Zhen, 2011). Representative traces of spontaneous mIPSCs and mEPSCs in wild-type animals are shown in (B). When held at -10 mV, both mIPSCs and mEPSCs were recorded, as outward and inward currents, respectively. Application of 0.5 mM D-tubocurarine (d-TBC) allowed for the isolation of mIPSC events, as it completely blocked mEPSCs. At -30 mV only mEPSCs were recorded (left bottom panel), since all events were blocked by 0.5 mM d-TBC (right bottom panel). Representative traces are shown in (C) with different timescales of spontaneous GABAergic mIPSCs in wild-type, *nlg-1(ok259)*, and transgenic *nlg-1(ok259)* mutants expressing NLG-1 under its endogenous promoter (*nlg-1* fosmid) or a muscle-specific promoter (*Phlh-1::NLG-1*). Muscles were held at -10 mV. In (D)–(F), both the frequency and amplitude of mIPSCs were significantly decreased in *nlg-1* mutants and were restored to wild-type levels by expressing NLG-1 under its endogenous promoter or a muscle-specific promoter. Representative traces of GABA (0.5 mM)-evoked currents at muscle cells are shown in (G). The peak amplitude and desensitization kinetics of GABA-evoked currents in *nlg-1* mutants (H) were comparable to that in wild-type animals. * $p < 0.05$; ns, not significant, by Mann-Whitney U test.

and postsynaptic scaffolding molecules like PSD-95, S-SCAM, and gephyrin (Pouloupoulos et al., 2009; Irie et al., 1997; Iida et al., 2004; Xu et al., 2010). It is unclear whether any of these interactions, alone or in concert, is necessary to form or maintain neuroigin clusters at postsynaptic sites in vivo. To investigate mechanisms for NLG-1 clustering at the postsynaptic NMJs, we first took a structure-function approach. We expressed NLG-1 deletion constructs that lack particular domains and analyzed their localization pattern. NLG-1, like its vertebrate homologs, is a single type I transmembrane protein with an extracellular cholinesterase-like domain and a small intracellular tail ending with a PDZ-binding

motif. To evaluate the importance of interactions through the PDZ-binding domain for NLG-1 localization, we first expressed a NLG-1::YFP construct that lacks the three most C-terminal amino acids. The corresponding NLG-1 Δ PDZBD::YFP protein showed normal, punctate localization apposite to the

GABAergic presynaptic terminals (Figure S1A). More surprisingly, we found that truncating the entire cytosolic tail (NLG-1 Δ intraC::YFP) did not alter the localization of NLG-1::YFP (Figure S1B). Moreover, the ability of NLG-1 Δ intraC::YFP to cluster normally was not due to dimerization with the endogenous NLG-1, since its localization was indistinguishable between wild-type and *nlg-1(ok259)* animals (Figures S1B and S1C). These results suggest that the recruitment of NLG-1 to inhibitory postsynaptic sites is entirely dependent on extracellular interactions. To further test this possibility, we expressed a truncated NLG-1 construct that retained the signal peptide directly followed by the extracellular YFP tag, the putative O-glycosylation region, as well as the transmembrane domain and cytosolic tail. The NLG-1 Δ extraC::YFP did not form any detectable clusters, but was instead diffusely distributed on the plasma membrane (Figure S1D). Together, these results strongly argue that NLG-1 clusters can form independently of postsynaptic scaffolding protein interaction, but rely on extracellular binding partner(s). We also tested the ability of these truncated forms of NLG-1 to cluster GABA_ARs. Not surprisingly, NLG-1 Δ extraC, which showed a diffuse distribution on the membrane, was unable to rescue the GABA_AR clustering defect of *nlg-1* mutants (Figure S1F). Interestingly, just removing the three-residue PDZ-binding motif at the C terminus of NLG-1 drastically compromised its ability to cluster GABA_ARs (Figure S1F). However, NLG-1 Δ intraC, which also clustered normally at inhibitory postsynapses, completely failed to rescue the GABA_AR clustering defects (Figure S1F), suggesting that other domains within the cytosolic tail of NLG-1 are necessary for GABA_AR recruitment. Together, this structure-function analysis shows that NLG-1 is recruited to GABAergic synapses via its extracellular domain and clusters GABA_ARs through its PDZ-binding motif and cytoplasmic tail.

The most likely *trans*-synaptic binding candidate for NLG-1 is the sole *C. elegans* neurexin ortholog, NRX-1, which has been reported to be expressed in most if not all *C. elegans* neurons (Haklai-Topper et al., 2011). The *C. elegans nrx-1* locus encodes a long and a short neurexin isoform (Figure 3B). The long isoform encodes proteins that are similar to α -neurexins in vertebrates with a single transmembrane domain and a large extracellular domain encompassing multiple laminin G and EGF-like domains. The shorter isoform is generated from an alternative internal promoter in the same locus. To test if NRX-1 clusters NLG-1, we introduced three analogous missense mutations in NLG-1 that are predicted to abolish its putative binding sites for β -neurexin (Araç et al., 2007) and expressed the corresponding protein, NLG-1(QED), in muscle cells of *nlg-1(ok259)* mutant animals. The localization of NLG-1(QED) apposite to GABAergic presynaptic terminals was indistinguishable from that of the wild-type NLG-1, suggesting that NRX-1 may not be essential or sufficient for NLG-1 clustering (Figure S1E).

It remained possible that these mutations may not completely abolish binding between the worm NLG-1 and NRX-1 proteins. Therefore, we next analyzed various *nrx-1* mutants. We analyzed two deletion alleles in the long *nrx-1* isoform, *ds1* and *ok1649*. *ok1649* has been reported to behave as a putative null for *nrx-1* function (Calahorra and Ruiz-Rubio, 2013). Both alleles also failed to show any detectable NLG-1 clustering

phenotype (Figure 3A). But because both alleles only affected the long isoform of *nrx-1*, it was possible that the short form contributed to NLG-1 clustering. To further eliminate NRX-1 function, we generated a large deletion in the *nrx-1* locus, *nrx-1(wy778)*, which encompasses the transmembrane and cytoplasmic domains shared by all NRX-1 isoforms and removes the short isoform entirely (Figure 3B). In animals carrying this allele, we found no significant reduction in the clustering or intensity of NLG-1::YFP puncta (Figures 3C, 3D, 3I, and 3J) and no obvious defect in UNC-49 clustering (Figures 4B, 4D, and 4E) when compared to wild-type animals. Active zones and synaptic vesicles also seemed to accumulate normally at presynaptic terminals in the *nrx-1(wy778)* mutant (Figure S2). Therefore, NRX-1 is likely dispensable for NLG-1 and GABA_AR clustering. These results imply that NLG-1 becomes specifically associated with inhibitory postsynaptic sites through additional extracellular interactions.

NLG-1 and GABA_AR Clustering Is Compromised in the Absence of Punctin/MADD-4 and NRX-1

A recent study showed that Punctin/MADD-4, an extracellular synaptic protein secreted from axonal terminals, is important for proper differentiation of cholinergic and GABAergic synapses (Pinan-Lucarré et al., 2014). The *madd-4* locus encodes a long (MADD-4L) and short (MADD-4S) isoform from putative distinct promoters. While the long form is specifically localized to the cholinergic postsynapse, the short form is present at both cholinergic and GABAergic synapses (Pinan-Lucarré et al., 2014). Consistent with this study, we found that MADD-4S::YFP exhibited a punctate localization pattern along the nerve cord; a portion of the MADD-4S puncta colocalized with the NLG-1 clusters at GABAergic synapses (Figure 3E). We then examined whether NLG-1 clustering was dependent on MADD-4 and found that NLG-1 puncta maximum fluorescence intensity was slightly reduced (–13%) compared to wild-type, while synaptic density was reduced by 40% (Figures 3F, 3I, and 3J).

To test if MADD-4 and NRX-1 act redundantly to cluster NLG-1, we examined the *madd-4; nrx-1* double mutant. In the absence of both genes, NLG-1::YFP becomes much more diffuse when compared to the *madd-4* single mutant (Figure 3G). A line scan analysis of the NLG-1::YFP signal showed that peak intensities in the double mutant were dramatically reduced when compared to wild-type animals (Figure 3H). We also found a dramatic decrease in synaptic density (–70%) as well as in the maximum synaptic fluorescence intensity (–38%) (Figures 3I and 3J). These results suggest that MADD-4 and NRX-1 play critical and largely redundant roles in clustering NLG-1 at postsynaptic specializations.

We next examined whether MADD-4 and NRX-1 are also required for GABA_AR clustering at the postsynaptic terminal. Using the UNC-49::YFP marker, we found that maximum puncta fluorescence intensity was not changed, but synaptic density was reduced by 25% in *madd-4* mutants (Figure 4E), which is consistent with our observations with the NLG-1::YFP marker. Strikingly, UNC-49::YFP no longer formed any visible clusters in the *madd-4(ok2854); nrx-1(wy778)* double mutant (Figure 4F) and appeared diffuse on the plasma membrane. Together, these results suggest that both NRX-1 and MADD-4 are responsible for

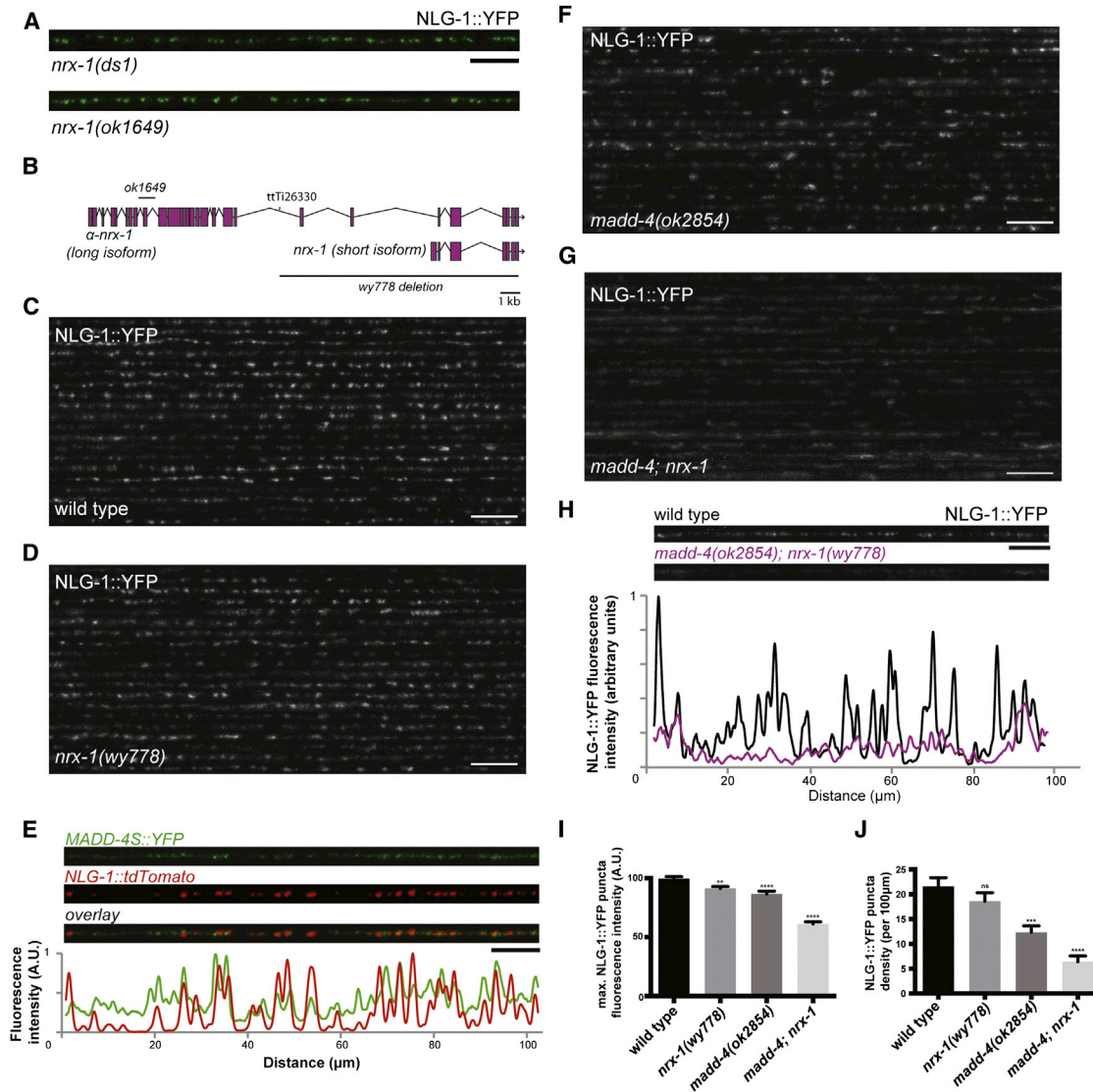


Figure 3. MADD-4 and NRX-1 Are Redundantly Required for NLG-1 Localization at the Synapse

(A) Confocal micrographs of *nrx-1(ds1)* and *nrx-1(ok1649)* mutant animals showing NLG-1::YFP clusters in the dorsal nerve cord.

(B) Schematic representation of the *nrx-1* locus, showing the α -neurexin and β -neurexin isoforms, the Mos transposon insertion site (ttTi26330), as well as the *ok1649* and *wy778* deletions.

(C and D) Confocal micrographs showing the dorsal nerve cord of 20 wild-type (C) and *nrx-1(wy778)* (D) animals expressing NLG-1::YFP.

(E) Confocal micrographs of neuronally secreted MADD-4S::YFP and muscle NLG-1::tdTomato at the dorsal nerve cord. The fluorescence profile of MADD-4S::YFP (green) and NLG-1::tdTomato (red), normalized to their respective maximum intensity, are shown.

(F and G) Confocal micrographs showing the dorsal nerve cord of 20 *madd-4(ok2854)* (F) and *madd-4(ok2854); nrx-1(wy778)* double (G) mutant animals.

(H) The fluorescence profiles of NLG-1::YFP in a wild-type and *madd-4(ok2854); nrx-1(wy778)* double mutant animal are shown. Both fluorescence profiles were normalized to the wild-type maximum intensity.

(I and J) Quantification of NLG-1::YFP puncta maximum fluorescence intensity (I) and synaptic density (J). An ANOVA and post hoc Tukey's tests were used to determine significant differences between the different genotypes. Error bars indicate SEM. p values are * < 0.05, *** < 0.001, **** < 0.0001. Scale bars: 5 μ m (A and E), 10 μ m (C, D, and F–H).

recruiting NLG-1 and GABA_ARs to the postsynaptic terminals. Neurexin has been well characterized as a presynaptic protein in vertebrate systems. However, it has also been reported to function on the postsynaptic side of NMJs in *C. elegans* (Hu et al., 2012). To determine if NRX-1 could act in GABAergic neurons, we used two overlapping fosmids spanning the entire *nrx-1*

locus and engineered a bicistronic GFP reporter at the 3'-end of *nrx-1*. The *nrx-1::SL2::GFP* transgene showed GFP expression in GABAergic neurons, as well as some other ventral cord motor neurons (Figure 4G). Furthermore, a GFP-tagged NRX-1 expressed in GABAergic neurons localized to presynaptic sites (Figure 4H). Finally, specific expression of a *nrx-1* minigene in

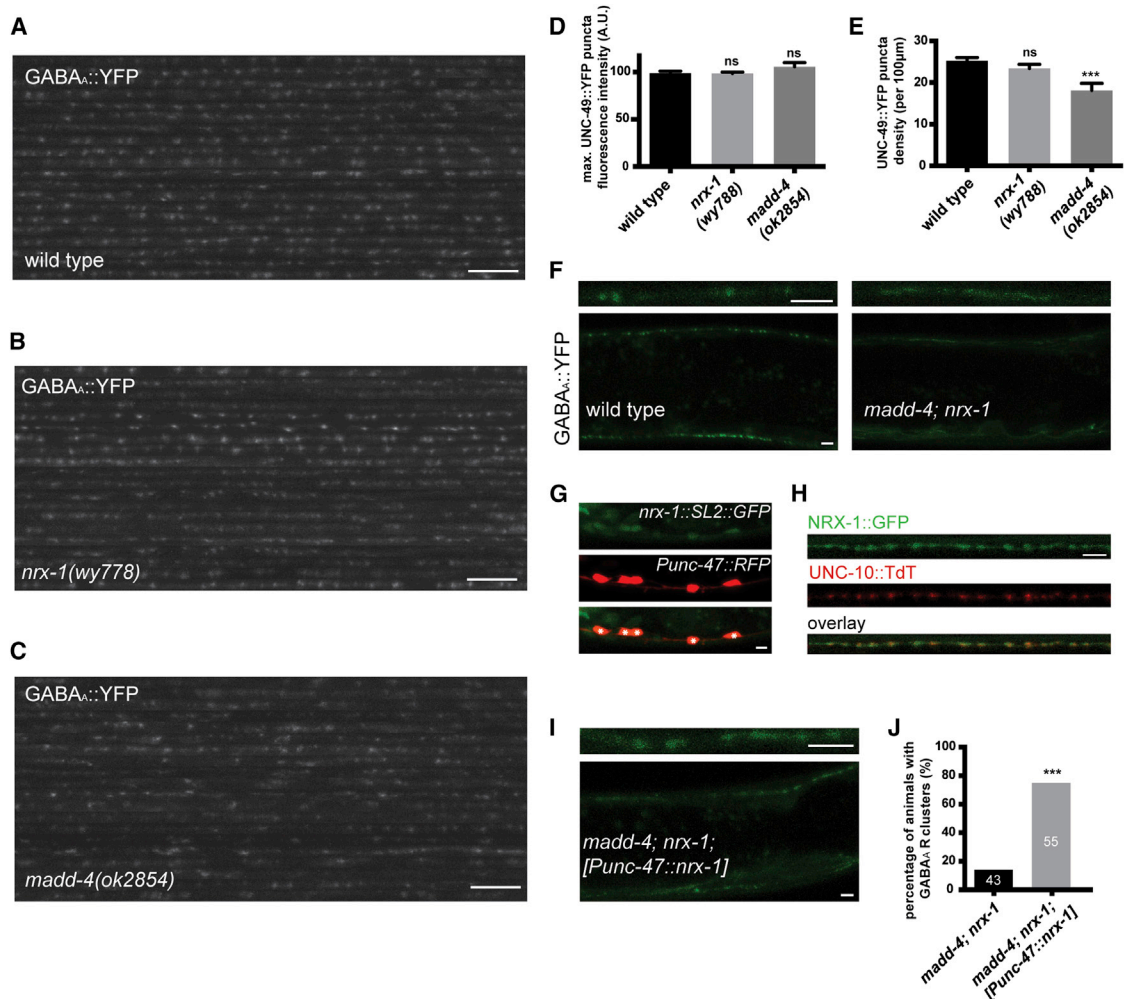


Figure 4. GABA_A Receptor Clustering Is Impaired in the Absence of MADD-4 and NRX-1

(A–C) Confocal micrographs showing the dorsal nerve cord of 20 wild-type (A), *nrx-1(wy778)* (B), and *madd-4(ok2854)* (C) mutant animals. (D and E) Quantification of UNC-49::YFP puncta maximum fluorescence intensity (D) and synaptic density (E) in wild-type, *nrx-1(wy778)*, and *madd-4(ok2854)* animals. An ANOVA and post hoc Tukey's tests were used to determine significant differences between the different genotypes. Error bars indicate SEM. p values are *** < 0.001. (F) Confocal micrographs showing the dorsal and ventral nerve cords of a wild-type and *madd-4; nrx-1* double mutant animal expressing UNC-49::YFP. Top panels show a higher magnification of the dorsal nerve cord. (G) A transgene carrying a genomic fragment of *nrx-1* fused to an SL2::GFP shows expression in GABAergic neurons, labeled in red (asterisks), as well as other ventral nerve cord neurons. (H) NRX-1::GFP localizes to inhibitory presynaptic sites, labeled with the active zone marker UNC-10::TdT. (I) Specific expression of a *nrx-1* minigene in GABAergic neurons induces GABA_AR clusters in *madd-4; nrx-1* double mutants. (J) Quantification of GABA_AR clustering in the *madd-4; nrx-1* double mutant in the absence or presence of NRX-1 in GABAergic neurons. p < 0.001, Fisher's exact test. Scale bar: 10 µm (A–C), 3 µm (F–I).

GABAergic motor neurons induced GABA_AR clusters in *madd-4; nrx-1* double mutants (Figures 4I and 4J). These data suggest that NRX-1 acts at presynaptic sites, in *trans* with NLG-1 on the muscle membrane, to cluster postsynaptic GABA_ARs.

To further characterize the role of MADD-4 and NRX-1 at GABAergic synapses, we recorded spontaneous inhibitory postsynaptic currents (mIPSCs) in the muscles of the *madd-4* and *nrx-1* single and the *madd-4; nrx-1* double mutant animals (Figure 5A). We found that both the frequency and amplitude of mIPSCs in *nrx-1* single mutants were similar to that of wild-

type animals (Figures 5B and 5C). The frequency of mIPSCs was moderately reduced in the *madd-4* single mutant, while the amplitude of mIPSCs was unchanged (Figures 5B and 5C). In *madd-4; nrx-1* double mutants, the mIPSC frequency was further and significantly reduced when compared to *madd-4* single mutants (Figure 5B). Importantly, the mIPSC amplitude was decreased in *madd-4; nrx-1* double mutants (Figure 5C), a phenotype shared by *nlg-1* mutants. A reduced mIPSC frequency could result from either reduced presynaptic release or decreased postsynaptic receptor numbers. Our NLG-1 and

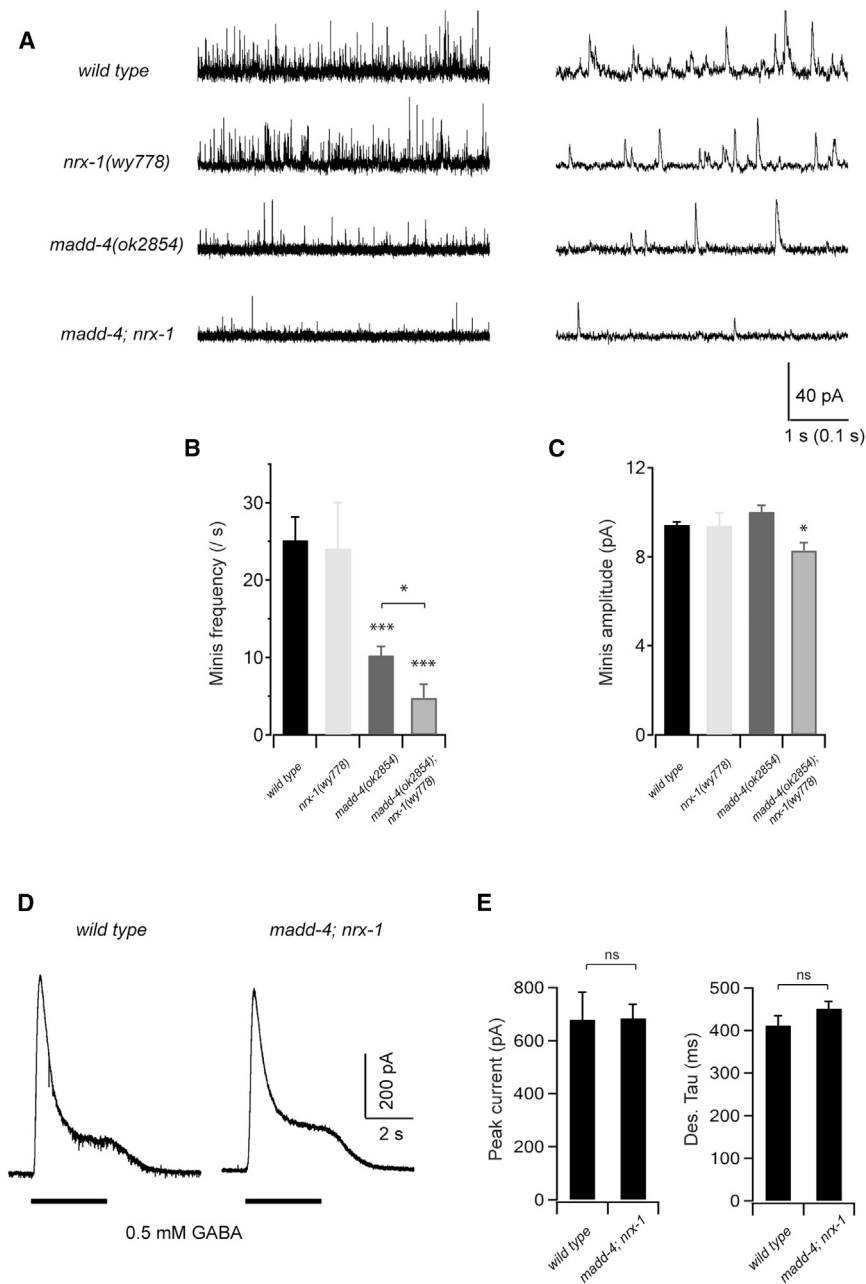


Figure 5. MADD-4 and NRX-1 Are Redundantly Required for GABAergic Synaptic Transmission

(A) Representative traces of spontaneous GABAergic mIPSCs in wild-type (WT) animals, as well as *nrx-1*, *madd-4*, and *madd-4; nrx-1* mutants with different timescales. Body wall muscles were held at -10 mV.

(B and C) Quantification of the frequency and amplitude of mIPSCs in various genetic backgrounds. Both frequency and amplitude were significantly decreased in *madd-4; nrx-1* double mutants, whereas only mIPSC frequency was decreased in *madd-4* single mutants. Neither frequency nor amplitude was significantly changed in *nrx-1* mutants when compared to wild-type animals.

(D) Representative traces of GABA (0.5 mM)-evoked currents at muscle cells.

(E) The peak amplitude and desensitization kinetics of GABA-evoked currents in *madd-4; nrx-1* double mutants were comparable to that in wild-type animals. * $p < 0.05$, *** $p < 0.001$; ns, not significant, by the Mann-Whitney U test.

and GABA_AR clustering analyses, these data strongly support the notion that MADD-4 acts together with NRX-1 to recruit NLG-1 and GABA_ARs to postsynaptic terminals.

Punctin/MADD-4 Biochemically Interacts with Both Neuroigin and Neurexin

To further test this hypothesis, we assayed the biochemical interactions between these three molecules using several approaches. First, we used a luciferase cell-based assay previously used to probe the interaction between MADD-4S and various receptors (Chan et al., 2014). To ask whether MADD-4S could directly interact with NLG-1, we expressed luciferase-tagged MADD-4S from HEK293T cells, collected the conditioned media, and applied it to HEK293T cells transfected with NLG-1::

GABA_AR clustering analyses (Figure 3 and Figure 4) as well as the muscle-specific requirement of NLG-1 to rescue GABAergic morphological defects (Figure 1 and Figure 2) point toward a functional contribution of reduced postsynaptic receptor density. To further assess if this is due to the dispersal or lack of the membrane GABA_ARs in *nrx-1; madd-4* mutants, we examined the evoked response in muscles upon exogenous GABA (0.5 mM) application. As was the case in the *nlg-1* mutants, the amplitude and kinetics of GABA-evoked currents were unchanged in the *madd-4; nrx-1* double mutants (Figures 5D and 5E), suggesting that the total number of muscle membrane GABA_ARs was unchanged. Together with our NLG-1

FLAG::GFP. Upon immunoprecipitation (IP) of the NLG-1::FLAG::GFP receptors, we identified a higher luciferase activity in the washed immunoprecipitate, suggesting an interaction between the two proteins (Figure 6C). Such an interaction was confirmed by co-immunoprecipitation (coIP) experiments between secreted MADD-4S::FLAG and NLG-1::GFP transfected in HEK293 cells (Figure 6D). Interestingly, using the luciferase assay, we found that the addition of secreted NRX-1[EGF3+LNS6] in the medium potentiated the observed binding between NLG-1 and MADD-4S::GLuc (Figure 6C), which raises the possibility that MADD-4S might also interact with NRX-1. We tested this hypothesis using the luciferase assay and found increased

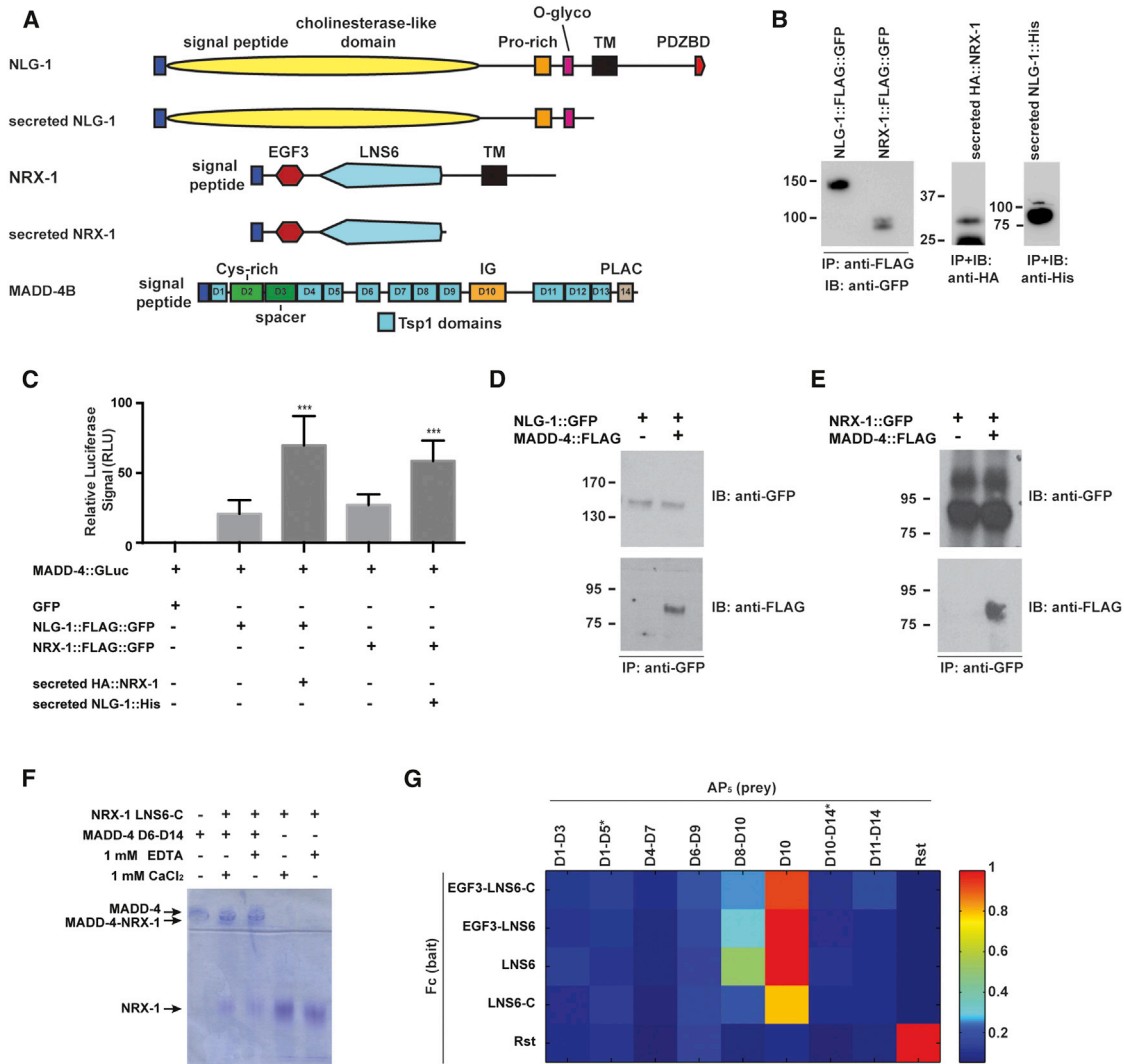


Figure 6. MADD-4S Interacts with NLG-1 and NRX-1

(A) Schematic representations of NLG-1, NRX-1, and MADD-4S constructs used in binding assays.

(B) Western blots showing immunoprecipitated proteins used for the luciferase binding assays. The western blot on the left shows the transmembrane NLG-1 and NRX-1; the western blots on the right show the secreted NRX-1 and NLG-1 collected from culture media.

(C) Normalized levels of MADD-4S::luciferase signal that immunoprecipitated with NLG-1::FLAG::GFP or NRX-1::FLAG::GFP in a HEK293T cell surface binding assay, in the absence or presence of secreted NRX-1 or NLG-1 ectodomains, respectively. An ANOVA and post hoc Tukey's tests were used to determine significant differences between the different conditions. *** $p < 0.001$.

(D) HEK293T cells were transfected with NLG-1::GFP and incubated with concentrated conditioned media containing MADD-4S::FLAG. MADD-4S::FLAG was pulled down when NLG-1::GFP was immunoprecipitated.

(E) HEK293T cells were transfected with NRX-1::GFP and incubated with concentrated conditioned media containing MADD-4S::FLAG. MADD-4S::FLAG was pulled down when NRX-1::GFP was immunoprecipitated.

(F) Native PAGE shift assay for NRX-1 and MADD-4S. The NRX-1 construct used includes the LNS6 domain and the unstructured region to its C terminus before the transmembrane helix (labeled as LNS6-C). NRX-1 and MADD-4S were used at 15 μ M.

(G) ECIA for various extracellular fragments of NRX-1 and MADD-4S. Binding is detected by absorbance at 650 nm. *Drosophila* Rst extracellular region was used as a negative control (against NRX-1 and MADD-4S) and a positive control as a hemophilic binder (lowest right corner). MADD-4S constructs with very poor expression are labeled with an asterisk. See Figure S3.

levels of luciferase activity associated with cells expressing NRX-1::FLAG::GFP (Figure 6C). Similar to our previous set of experiments, adding the extracellular domain of NLG-1 in the medium increased the observed interaction between NRX-1 and MADD-4S (Figure 6C). The direct interaction between

NRX-1 and MADD-4S was confirmed by coIP experiments (Figure 6E).

We applied native polyacrylamide gel shift assays using purified proteins to further dissect the physical interaction between MADD-4S and NRX-1. We created constructs of MADD-4S

for expression in insect cells using baculoviruses and transient transfections. While we could not produce monodisperse full-length MADD-4S in appreciable quantities, we could produce parts of MADD-4S (Figure 6F). We observed that domains 6–14 of MADD-4S bind to the LNS6 domain of NRX-1 using native polyacrylamide gel shifts (Figure 6F). MADD-4S is a heavily positively charged protein (pI: 8.8) and does not migrate in a native gel toward the anode (Figure 6F, lane 1). Neurexin is an acidic protein (pI: 5.6) and migrates rapidly toward the anode (Figure 6F, lanes 4 and 5). When mixed together at 15 μ M, most of the free neurexin and MADD-4S disappears and a new band appears representing the complex (pI: 8.4 assuming a 1:1 complex) (Figure 6F, lanes 2 and 3). Complex formation is not dependent on the presence of Ca^{2+} or EDTA.

We further probed this binding using an avidity-based binding assay designed for extracellular proteins, called the Extracellular Interactome Assay (ECIA) (Özkan et al., 2014). Fc-tagged neurexin (bait) produced in *Drosophila* S2 cells was captured on Protein A-coated microplates, which were incubated with alkaline phosphatase-tagged, pentamerized MADD-4S fragments as prey. Binding between bait and prey was detected using a colorimetric alkaline phosphatase substrate. Several MADD-4S constructs could produce detectable amounts of protein (Figure S3), and we could see that moderately expressing MADD-4S fragments of domains 8–10 and domain 10 (immunoglobulin) alone interact with all NRX-1 fragments containing the LNS6 domain (Figure 6G). Hence, the native gel shift assays and the ECIA demonstrate a direct interaction between the LNS6 domain of NRX-1 and the immunoglobulin domain of MADD-4S.

Together, our protein interaction data suggest a model whereby NRX-1 and MADD-4S cooperate to recruit NLG-1 through direct interactions within a NLG-1/MADD-4S/NRX-1 tripartite complex.

DISCUSSION

We set out to determine the localization and function of the *C. elegans* neuroligin ortholog at NMJs. Our results indicate that in muscles NLG-1 is specifically associated with inhibitory postsynapses and that it is involved in the synaptic clustering of GABA_ARs. Consistent with these findings, *nlg-1* mutants show defects in spontaneous inhibitory postsynaptic currents.

Mammalian neuroligin family members NL1 and NL2 show preferential association with excitatory and inhibitory postsynapses, respectively (Song et al., 1999; Varoqueaux et al., 2004). This raised the intriguing possibility that neuroligins might define the chemical subtype of specific synapses. We were interested in determining the localization pattern of the sole neuroligin family member in *C. elegans*, NLG-1. The NMJ represents a very suitable system to address this question, since both excitatory cholinergic and inhibitory GABAergic postsynaptic sites are present in muscle cells, they intercalate with one another along the dorsal and ventral nerve cords, and their position can be inferred from the localization of corresponding presynaptic sites. A generic postsynaptic localization could be suggestive of an ancestral role for neuroligin as a synaptic adhesion molecule that is diversified in higher organisms. In contrast, we found that NLG-1 shows exquisite specificity for GABAergic postsynapses, and is absent from excitatory cholinergic postsynaptic

sites. This suggests that the worm NLG-1 is functionally most analogous to the vertebrate NL2.

What could be the mechanisms that ensure specific localization of NLG-1 at inhibitory postsynapses? Mammalian NL2 has been shown to interact with two components of inhibitory postsynaptic scaffolds, gephyrin and collybistin (Pouloupoulos et al., 2009). However, the localization of NL2 is mostly unaltered in cerebellar Purkinje cells of GABA_A α 1 knockout mice (Patrizi et al., 2008), which subsequently lack gephyrin aggregates, or in collybistin knockout hippocampal neurons (Pouloupoulos et al., 2009), which lack all three postsynaptic molecules, suggesting that NL2 clustering lies fairly upstream in the sequence of events leading to postsynaptic assembly. The situation in *C. elegans* is likely to be similar, since our results show that while NLG-1 is required for GABA_AR UNC-49 clustering, its own clustering is independent of UNC-49. In fact, no collybistin ortholog is predicted from the *C. elegans* genome, and to the best of our knowledge, no synaptic function has been identified to date for the gephyrin ortholog *moc-1* and paralog *lin-46*. Besides arguing against a role for postsynaptic scaffold molecules in determining NLG-1 localization, these observations also raise the question as to how NLG-1 recruits GABA_ARs. Our analysis of truncated versions of NLG-1 suggests that proteins interacting with its PDZ-binding domain and its cytoplasmic tail might mediate this function.

Our structure-function analysis of NLG-1, together with the examination of various mutant alleles of *nrx-1*, strongly supported the idea that NLG-1 relied on extracellular cues other than NRX-1 for its localization. We found that Punctin/MADD-4, an extracellular synaptic protein secreted from axonal terminals implicated in synaptic differentiation (Pinan-Lucarré et al., 2014), plays important roles in clustering NLG-1 and GABA_ARs. Furthermore, three lines of evidence support the notion that Punctin/MADD-4 acts synergistically with NRX-1 to recruit NLG-1. First, while the *nrx-1* mutant showed no defects in NLG-1 or GABA_AR clustering, *madd-4* mutants have a reduced number of clusters, a phenotype that is significantly enhanced in *madd-4; nrx-1* double mutants. Second, our electrophysiological recordings showed a reduced frequency of miniature inhibitory postsynaptic current in *madd-4* single mutant, which is also significantly enhanced in the *madd-4; nrx-1* double mutant. Third, we found that MADD-4S directly interacts with both NLG-1 and NRX-1 and that the three molecules seem to bind to one another in a cooperative manner. Together, these pieces of evidence strongly argue that MADD-4 plays an essential role in clustering NLG-1 and GABA_AR at postsynaptic specializations. Surprisingly, MADD-4's function seems more important than NRX-1's, since few defects can be detected in the *nrx-1* single mutant. The fact that *madd-4; nrx-1* double mutant showed almost completely diffuse GABA_AR and NLG-1 at the plasma membrane, as well as dramatically reduced mini-IPSC, indicates that these two proteins together account for the majority of postsynaptic organizing activities.

A companion paper by Tu et al. (2015) found similar roles for MADD-4S in recruiting NLG-1 to the postsynaptic sites of GABAergic synapses. They also report that MADD-4S binds to UNC-40/DCC, another receptor required for clustering GABA_ARs at inhibitory postsynaptic specializations. Together

with the lack of obvious behavioral defects in *nlg-1* mutants, these results indicate that there might be multiple parallel molecular pathways to recruit NLG-1 and postsynaptic receptors. Binding between MADD-4S and NRX-1 or UNC-40 argue that there might be crosstalk between some of these pathways.

Do similar mechanisms exist in other organisms? While a large body of literature supports the model that mammalian neuroligins and neuroligins are synaptic adhesion pairs that specify the function and development of various types of synapses, the genetic relationships between the various NLs and neuroligins are unclear due to the high level of redundancy in both gene families. This question has been best addressed in fruit flies. Loss of function of either *dNlg1* or *dNrx* causes similar synaptic defects (Banovic et al., 2010). Interestingly, the *dNlg1* mutant phenotypes are quantitatively stronger compared with the *dNrx* mutants, suggesting that factors such as *Punctin/Madd-4* may play a role. Supporting this notion is the observation that *dNrx* binding is not absolutely required for *dNlg1* function (Banovic et al., 2010). Whether the *Drosophila* *Punctin* is also necessary to cluster and activate *dNlg1* remains to be tested. Another possible ligand for neuroligin is thrombospondin, as suggested by an in vitro study (Xu et al., 2010).

A previous study showed that NRX-1 and NLG-1 are required for a retrograde signal that inhibits synaptic vesicle release at the cholinergic synapses (Hu et al., 2012). The authors found that NRX-1 functions in the muscles while NLG-1 functions in the cholinergic neurons. The defect in retrograde signaling is only induced in the *mir-1* mutant background. However, no synaptic release phenotype was reported in the single mutant phenotype. Hence, there is no obvious inconsistency between the role of NLG-1 at GABAergic postsynapses and its role at presynaptic terminals of cholinergic neurons.

We describe here a mechanism that clusters neurotransmitter receptors locally to achieve the precise apposition between pre- and postsynaptic specializations. MADD-4S is secreted from the inhibitory presynaptic terminal and deposited locally at the ECM near synapses. Together with the presynaptic adhesion molecule NRX-1, MADD-4S enriches NLG-1 at postsynaptic sites, which in turn clusters GABA_ARs (Figure S4). Hence, the GABA presynaptic terminals organize postsynaptic differentiation through the action of both synaptic adhesion molecules and secreted ECM proteins. Finally, this study suggests that the *C. elegans* NMJ could represent a powerful model system to identify new ligands for neuroligin.

EXPERIMENTAL PROCEDURES

Constructs and detailed cloning information are available upon request.

Strains and Genetics

Wild-type animals were of Bristol variety N2 strain. Strains were maintained using standard methods at 20°C.

Transgenic Lines

Lines used in this study were as follows: *wyEx5982* (*Punc-47::mCherry::rab-3; Punc-129ΔBstEII::nlg-1::yfp; Podr-1::dsred*), *wyEx5983* (*Punc-129::mCherry::rab-3; Punc-129ΔBstEII::nlg-1::yfp; Podr-1::dsred*), *wyEx5984* (*Pmig-13::mCherry::rab-3; Punc-129ΔBstEII::nlg-1::yfp; Podr-1::dsred*), *wyEx4310* (*Punc-129ΔBstEII::nlg-1; Podr-1::GFP*), *wyEx5284* (*WRM0610dD09 nlg-1 fosmid; Podr-1::GFP*), *wyEx5333* (*Phlh-1::nlg-1; Podr-1::GFP*), *wyEx5516*

(*Punc-47::nlg-1::CFP; odr-1::GFP*), *wyEx7279* (*Punc-47::madd-4S::yfp; Punc-129ΔBstEII::nlg-1::tdTomato; Podr-1::gfp*), *wyEx4590* (*Punc-129ΔBstEII::nlg-1::YFPΔextraC; Podr-1::GFP*), *wyEx4592* (*Punc-129ΔBstEII::nlg-1::YFPΔPDZBD; Podr-1::GFP*), *wyEx4593* (*Punc-129ΔBstEII::nlg-1::YFPΔintraC; Podr-1::GFP*), *wyEx7987* (*Punc-129ΔBstEII::nlg-1ΔextraC; Podr-1::dsred*), *wyEx7988* (*Punc-129ΔBstEII::nlg-1ΔPDZBD; Podr-1::dsred*), *wyEx7989* (*Punc-129ΔBstEII::nlg-1ΔintraC; Podr-1::dsred*), *wyEx7990* (*Punc-47::nrx-1; Podr-1::dsred*), *wyEx8021* (*Punc-47::nrx-1::GFP; Punc-47::unc-10::TdT; Podr-1::GFP*), *krls1* (*Punc-47::SNB-1::CFP; unc-49p::unc-49::YFP; lin-15+*) *V*, and *wyls292* (*Punc-47::unc-10::tdTomato; Punc-129ΔBstEII::nlg-1::yfp; Podr-1::dsred*) *III*.

Mutants

Mutants used in this study were as follows: LGI, *madd-4*(OK2854); LGIII, *unc-119*(ed3); *unc-49*(e382); LGV, *ttT26330*; *nrx-1*(ds1); *nrx-1*(ok1649); *nrx-1*(wy778::unc-119+); LGX, *nlg-1*(ok259).

nrx-1 Deletion Mutant

We generated a large deletion in the *nrx-1* locus using MosDel (Frøkjær-Jensen et al., 2010). We obtained the IE26330 strain, which carries a Mos transposon insertion in an α -specific intron of *nrx-1* (Figure 4B), from the NEMAGENETAG consortium (Vallin et al., 2012). We designed a deletion cassette that contains an *unc-119* rescuing construct, flanked by approximately 2 kb of genomic sequence upstream of the *ttT26330* insertion site, and approximately 3 kb of genomic sequence downstream of the *nrx-1* STOP codon. The sequence encoding part of the extracellular domain of the long isoform is still present, but the deletion leads to a truncation of all α isoforms before the transmembrane domain and to an absence of the short isoform. The resulting deletion (*wy778::unc-119+*) spans a total of 12 kilobases, from the *ttT26330* insertion site to the STOP codon of the *nrx-1* locus, is replaced with an *unc-119* rescuing cassette, and was verified by long-range PCR using primers annealing outside of the deletion cassette.

Fluorescence Microscopy

Images of fluorescently tagged fusion proteins were captured in live L4 *C. elegans* using a Plan-Apochromat 40x/1.3 III objective on a Zeiss LSM710 confocal microscope. Worms were immobilized using a mixture of 225 mM 2,3-butanedione monoxime (Sigma-Aldrich) and 2.5 mM levamisole (Sigma-Aldrich) in 10 mM Na HEPES.

Confocal montages of dorsal nerve cords were assembled by imaging 20 L4 hermaphrodites of similar size in the mid-body region using identical image and laser settings for each genotype. Straightened dorsal cords were extracted from these images using the “straighten to line function” in the EMBL suite of ImageJ.

For quantifying NLG-1::YFP intensity along dorsal nerve cords, background fluorescence was first subtracted by calculating the average intensity of each image in a region devoid of NLG-1::YFP puncta. Fluorescence intensities along the cord were calculated using the “plot profile” function of ImageJ, and the 95th percentile and 5th percentile were determined for each genotype. Synapse numbers were calculated using the “analyze particles” function, with an intensity threshold of 20 and a puncta size threshold of 10 pixels.

Electrophysiology

The dissection of *C. elegans* animals was described previously (Richmond and Jorgensen, 1999). Briefly, 1-day-old hermaphrodite adults were glued to a sylgard-coated cover glass covered with bath solution. The integrity of the anterior ventral body muscle and the ventral nerve cord were visually examined via DIC microscopy, and anterior muscle cells were patched using fire-polished 4–6 M Ω -resistant borosilicate pipettes (World Precision Instruments). Membrane currents were recorded in the whole-cell configuration by a Digidata 1440A and a MultiClamp 700A amplifier, using the Clampex 10 software and processed with Clampfit 10 (Axon Instruments, Molecular Devices). Data were digitized at 10–20 kHz and filtered at 2.6 kHz.

The recording solutions were as described in our previous studies (Gao and Zhen, 2011). Specifically, the pipette solution contains the following: K-

gluconate, 115 mM; KCl, 25 mM; CaCl₂, 0.1 mM; MgCl₂, 5 mM; BAPTA, 1 mM; HEPES, 10 mM; Na₂ATP, 5 mM; Na₂GTP, 0.5 mM; cAMP, 0.5 mM; cGMP, 0.5 mM, at pH 7.2 with KOH, ~320 mOsm. The bath solution consists of the following: NaCl, 150 mM; KCl, 5 mM; CaCl₂, 5 mM; MgCl₂, 1 mM; glucose, 10 mM; sucrose, 5 mM; HEPES, 15 mM, at pH 7.3 with NaOH, ~330 mOsm. Under these conditions, the reversal potentials are ~-30 mV and ~+20 mV for GABA and ACh receptors, respectively. To isolate mIPSC events, recordings were performed with a holding potential of -10mV, with 0.5 mM D-tubocurarine (d-TBC) included in the bath solution to block all acetylcholine receptors. γ -Aminobutyric acid (GABA, 0.5 mM) and control/wash solutions were puffed onto patched muscle cells using a perfusion system (VC-66CST Teflon Valve System, Warner Instruments) to obtain evoked GABA currents. All chemicals were from Sigma. Experiments were performed at room temperatures (20°C–22°C).

Statistical Analysis for Electrophysiology

Two-tailed Mann-Whitney U test was used to compare the difference of the electrophysiological datasets. $p < 0.05$ was considered statistically significant. Subsequent analysis and graphing were performed using Excel (Microsoft), Igor Pro (Wavemetrics), and Clampfit (Molecular Devices). In this study, n refers to the number of recordings (one cell per animal). All data are presented as mean \pm SEM.

HEK293T Cell Surface Binding Experiments

The constructs used for cell transfections were pPRGS827 (pCDNA3-SS::HA::MADD-4S::Gaussia Luciferase [GLC], obtained from P. Roy [Chan et al., 2014]), pGM449 (pCMV::NLG-1::TM::FLAG::GFP), pGM451 (pCDNA3-SS::HA::NRX-1[EGF3+LNS6]), pGM467 (pCMV::NLG-1::His), pGM469 (pCDNA3-SS::HA::NRX-1[EGF3+LNS6]::TM::FLAG::GFP), pGM447 (pCMV::NLG-1::His::TM::GFP), pGM472 (pCMV::NLG-1::TM::GFP), and pGM464 (pCDNA3-SS::HA::MADD-4S::FLAG).

Cell surface Gaussia Luciferase binding assays were performed as previously described (Chan et al., 2014). To obtain concentrated conditioned culture media containing HA::MADD-4S::Gluc or NRX-1[EGF3+LNS6], 10 μ g of each respective expression plasmid was transfected into HEK293T cells on 10-cm dishes, and culture media was changed to DMEM-0.2% FBS. After 24 hr of culture, the conditioned media was collected and centrifuged to remove cellular debris and subsequently concentrated ten times using Pierce Protein concentrators 9K MWCO (Thermo Scientific). For the cell surface binding assays, 2 μ g of plasmid expressing NLG-1::FLAG was transfected into HEK293T cells in 6-well plates. Forty-eight hours post-transfection, culture media was removed and cells were incubated with concentrated conditioned media for 4 hr at 4°C. Cells were then harvested in a solution containing PBS, 0.2% BSA, and a protease inhibitor cocktail (PIC, Sigma) and lysed in TNTE buffer (50 mM Tris, 150 mM NaCl, 1 mM EDTA, 10 mM NaF, 1 mM Na₃VO₄, PIC, 0.5% Triton X-100) containing protease inhibitors. NLG-1::FLAG and NRX-1::FLAG were immunoprecipitated using anti-FLAG EZview affinity gel (Sigma), washed twice in lysis buffer, and then five times in TNTE buffer containing 0.1% Triton X-100 plus protease inhibitor. Half of the immunoprecipitate was taken for Gaussia Luciferase assays by using the BioLux Kit (NEB) and Synergy Neo Multi-Mode reader (BioTek). The other half was analyzed by western blot for quantification of proteins.

For colP experiments, the same protocol was used with the following modifications. Receptors were transfected into HEK293T cells in 10-cm dishes. Secreted ligands were concentrated using VivaSpin protein concentrators 5K MWCO (VivaScience). One milligram of protein from each reaction was immunoprecipitated with anti-GFP-bound agarose beads (Chromotek) for 2 hr at 4°C. Blots were incubated with an anti-GFP antibody (Roche) to assess receptor levels and an anti-FLAG antibody (Sigma) to detect MADD-4S.

NRX-1/MADD-4S Binding and Gel Shift Assays

Native gel shift assays were done using 4%–15% PhastGels on a PhastSystem using native buffer strips (pH 8.8, GE Healthcare). Samples were run for approximately 200 accumulated Volt*hours. Proteins for this assay were expressed using baculovirus-infected High Five cells. ECIA was performed

as explained in Özkan et al., 2014, with proteins produced in S2 cells using transient transfections.

SUPPLEMENTAL INFORMATION

Supplemental Information includes four figures and can be found with this article online at <http://dx.doi.org/10.1016/j.neuron.2015.05.015>.

AUTHOR CONTRIBUTIONS

G.S.M. designed and performed genetics, cell biology, and biochemistry experiments; collected and analyzed data; and wrote the manuscript. S.G. designed and performed electrophysiology experiments and collected and analyzed data and wrote the manuscript. A.M.O. performed the in vitro binding assays. W.L.H. performed biochemistry experiments and M.L. performed genetics experiments. E.O. and M.Z. helped design and oversee experiments. K.S. helped design, analyze, and oversee experiments and wrote the manuscript.

ACKNOWLEDGMENTS

Some strains were provided by the CGC, which is funded by NIH Office of Research Infrastructure Programs (P40 OD010440). Mos mutant strains were generated by the Ewbank and Ségalat labs as part of the NEMAGENETAG project funded by the European Community. They were distributed by M. Carre-Pierrat at the UMS 3421, supported by the CNRS. We thank Kevin Chan and Peter Roy for the pPRGS827 construct, as well as for advice on luciferase assays. We also thank J.L. Bessereau for the krls1 strain. This work is supported by the Canadian Institutes of Health Research (MOP 123250 and 93619) and NSERC (262112-12) (M.Z.), the Howard Hughes Medical Institute (K.S.), the Stanford Institute for Neuro-Innovation and Translational Neurosciences (SINTN) (K.S.), and the NINDS of the National Institutes of Health under award number 5R01NS048392 (K.S.).

Received: November 4, 2014

Revised: April 7, 2015

Accepted: May 1, 2015

Published: May 28, 2015

REFERENCES

- Araç, D., Boucard, A.A., Ozkan, E., Strop, P., Newell, E., Südhof, T.C., and Brunker, A.T. (2007). Structures of neuroligin-1 and the neuroligin-1/neurexin-1 beta complex reveal specific protein-protein and protein-Ca²⁺ interactions. *Neuron* 56, 992–1003.
- Bamber, B.A., Beg, A.A., Twyman, R.E., and Jorgensen, E.M. (1999). The *Caenorhabditis elegans* unc-49 locus encodes multiple subunits of a heteromultimeric GABA receptor. *J. Neurosci.* 19, 5348–5359.
- Banovic, D., Khorramshahi, O., Oswald, D., Wichmann, C., Riedt, T., Fouquet, W., Tian, R., Sigrist, S.J., and Aberle, H. (2010). *Drosophila* neuroligin 1 promotes growth and postsynaptic differentiation at glutamatergic neuromuscular junctions. *Neuron* 66, 724–738.
- Calahorra, F., and Ruiz-Rubio, M. (2013). Human alpha- and beta-NRXN1 isoforms rescue behavioral impairments of *Caenorhabditis elegans* neurexin-deficient mutants. *Genes Brain Behav.* 12, 453–464.
- Chan, K.K.M., Seetharaman, A., Bagg, R., Selman, G., Zhang, Y., Kim, J., and Roy, P.J. (2014). EVA-1 functions as an UNC-40 Co-receptor to enhance attraction to the MADD-4 guidance cue in *Caenorhabditis elegans*. *PLoS Genet.* 10, e1004521.
- Dean, C., Scholl, F.G., Choih, J., DeMaria, S., Berger, J., Isacoff, E., and Scheiffele, P. (2003). Neurexin mediates the assembly of presynaptic terminals. *Nat. Neurosci.* 6, 708–716.
- Frøkjær-Jensen, C., Davis, M.W., Hollopeter, G., Taylor, J., Harris, T.W., Nix, P., Lofgren, R., Prestgard-Duke, M., Bastiani, M., Moerman, D.G., and Jorgensen, E.M. (2010). Targeted gene deletions in *C. elegans* using transposon excision. *Nat. Methods* 7, 451–453.

- Gally, C., and Bessereau, J.-L. (2003). GABA is dispensable for the formation of junctional GABA receptor clusters in *Caenorhabditis elegans*. *J. Neurosci.* *23*, 2591–2599.
- Gao, S., and Zhen, M. (2011). Action potentials drive body wall muscle contractions in *Caenorhabditis elegans*. *Proc. Natl. Acad. Sci. USA* *108*, 2557–2562.
- Graf, E.R., Zhang, X., Jin, S.-X., Linhoff, M.W., and Craig, A.M. (2004). Neurexins induce differentiation of GABA and glutamate postsynaptic specializations via neuroligins. *Cell* *119*, 1013–1026.
- Haklai-Topper, L., Soutschek, J., Sabanay, H., Scheel, J., Hobert, O., and Peles, E. (2011). The neurexin superfamily of *Caenorhabditis elegans*. *Gene Expr. Patterns* *11*, 144–150.
- Hu, Z., Hom, S., Kudze, T., Tong, X.-J., Choi, S., Aramuni, G., Zhang, W., and Kaplan, J.M. (2012). Neurexin and neuroligin mediate retrograde synaptic inhibition in *C. elegans*. *Science* *337*, 980–984.
- Hunter, J.W., Mullen, G.P., McManus, J.R., Heatherly, J.M., Duke, A., and Rand, J.B. (2010). Neuroligin-deficient mutants of *C. elegans* have sensory processing deficits and are hypersensitive to oxidative stress and mercury toxicity. *Dis. Model. Mech.* *3*, 366–376.
- Ichtkenko, K., Hata, Y., Nguyen, T., Ullrich, B., Missler, M., Moomaw, C., and Südhof, T.C. (1995). Neuroligin 1: a splice site-specific ligand for beta-neurexins. *Cell* *81*, 435–443.
- Iida, J., Hirabayashi, S., Sato, Y., and Hata, Y. (2004). Synaptic scaffolding molecule is involved in the synaptic clustering of neuroligin. *Mol. Cell. Neurosci.* *27*, 497–508.
- Irie, M., Hata, Y., Takeuchi, M., Ichtkenko, K., Toyoda, A., Hirao, K., Takai, Y., Rosahl, T.W., and Südhof, T.C. (1997). Binding of neuroligins to PSD-95. *Science* *277*, 1511–1515.
- Li, J., Ashley, J., Budnik, V., and Bhat, M.A. (2007). Crucial role of *Drosophila* neurexin in proper active zone apposition to postsynaptic densities, synaptic growth, and synaptic transmission. *Neuron* *55*, 741–755.
- McIntire, S.L., Jorgensen, E., and Horvitz, H.R. (1993). Genes required for GABA function in *Caenorhabditis elegans*. *Nature* *364*, 334–337.
- Nishimune, H., Sanes, J.R., and Carlson, S.S. (2004). A synaptic laminin-calcium channel interaction organizes active zones in motor nerve terminals. *Nature* *432*, 580–587.
- Özkan, E., Chia, P.H., Wang, R.R., Goriatcheva, N., Borek, D., Otwinowski, Z., Walz, T., Shen, K., and Garcia, K.C. (2014). Extracellular architecture of the SYG-1/SYG-2 adhesion complex instructs synaptogenesis. *Cell* *156*, 482–494.
- Patrizi, A., Scelfo, B., Viltono, L., Briatore, F., Fukaya, M., Watanabe, M., Strata, P., Varoqueaux, F., Brose, N., Fritschy, J.-M., and Sassoè-Pognetto, M. (2008). Synapse formation and clustering of neuroligin-2 in the absence of GABA_A receptors. *Proc. Natl. Acad. Sci. USA* *105*, 13151–13156.
- Pinan-Lucarré, B., Tu, H., Pierron, M., Cruceyra, P.I., Zhan, H., Stigloher, C., Richmond, J.E., and Bessereau, J.-L. (2014). *C. elegans* Punctin specifies cholinergic versus GABAergic identity of postsynaptic domains. *Nature* *511*, 466–470.
- Pouloupoulos, A., Aramuni, G., Meyer, G., Soykan, T., Hoon, M., Papadopoulos, T., Zhang, M., Paarmann, I., Fuchs, C., Harvey, K., et al. (2009). Neuroligin 2 drives postsynaptic assembly at perisomatic inhibitory synapses through gephyrin and collybistin. *Neuron* *63*, 628–642.
- Richmond, J.E., and Jorgensen, E.M. (1999). One GABA and two acetylcholine receptors function at the *C. elegans* neuromuscular junction. *Nat. Neurosci.* *2*, 791–797.
- Rothwell, P.E., Fuccillo, M.V., Maxeiner, S., Hayton, S.J., Gokce, O., Lim, B.K., Fowler, S.C., Malenka, R.C., and Südhof, T.C. (2014). Autism-associated neuroligin-3 mutations commonly impair striatal circuits to boost repetitive behaviors. *Cell* *158*, 198–212.
- Sanes, J.R., and Lichtman, J.W. (1999). Development of the vertebrate neuromuscular junction. *Annu. Rev. Neurosci.* *22*, 389–442.
- Siddiqui, T.J., and Craig, A.M. (2011). Synaptic organizing complexes. *Curr. Opin. Neurobiol.* *21*, 132–143.
- Song, J.Y., Ichtkenko, K., Südhof, T.C., and Brose, N. (1999). Neuroligin 1 is a postsynaptic cell-adhesion molecule of excitatory synapses. *Proc. Natl. Acad. Sci. USA* *96*, 1100–1105.
- Südhof, T.C. (2008). Neuroligins and neurexins link synaptic function to cognitive disease. *Nature* *455*, 903–911.
- Tu, H., Pinan-Lucarré, B., Ji, T., Jospin, M., and Bessereau, J.-L. (2015). *C. elegans* Punctin Clusters GABA_A Receptors via Neuroligin Binding and UNC-40/DCC Recruitment. *Neuron* *86*, this issue, 1407–1419.
- Vallin, E., Gallagher, J., Granger, L., Martin, E., Belougne, J., Maurizio, J., Duverger, Y., Scaglione, S., Borrel, C., Cortier, E., et al. (2012). A genome-wide collection of Mos1 transposon insertion mutants for the *C. elegans* research community. *PLoS ONE* *7*, e30482.
- Varoqueaux, F., Jamain, S., and Brose, N. (2004). Neuroligin 2 is exclusively localized to inhibitory synapses. *Eur. J. Cell Biol.* *83*, 449–456.
- Varoqueaux, F., Aramuni, G., Rawson, R.L., Mohrmann, R., Missler, M., Gottmann, K., Zhang, W., Südhof, T.C., and Brose, N. (2006). Neuroligins determine synapse maturation and function. *Neuron* *51*, 741–754.
- Xu, J., Xiao, N., and Xia, J. (2010). Thrombospondin 1 accelerates synaptogenesis in hippocampal neurons through neuroligin 1. *Nat. Neurosci.* *13*, 22–24.

Neuron, Volume 86

Supplemental Information

**MADD-4/Punctin and Neurexin
Organize *C. elegans* GABAergic
Postsynapses through Neuroligin**

Géraldine S. Maro, Shangbang Gao, Agnieszka M. Olechwiec, Wesley L. Hung, Michael Liu,
Engin Özkan, Mei Zhen, and Kang Shen

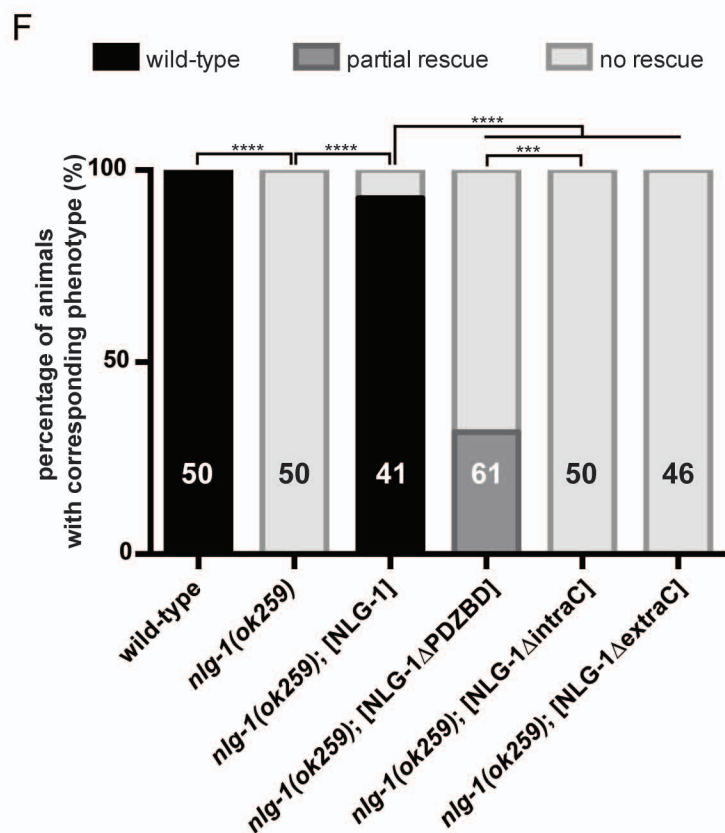
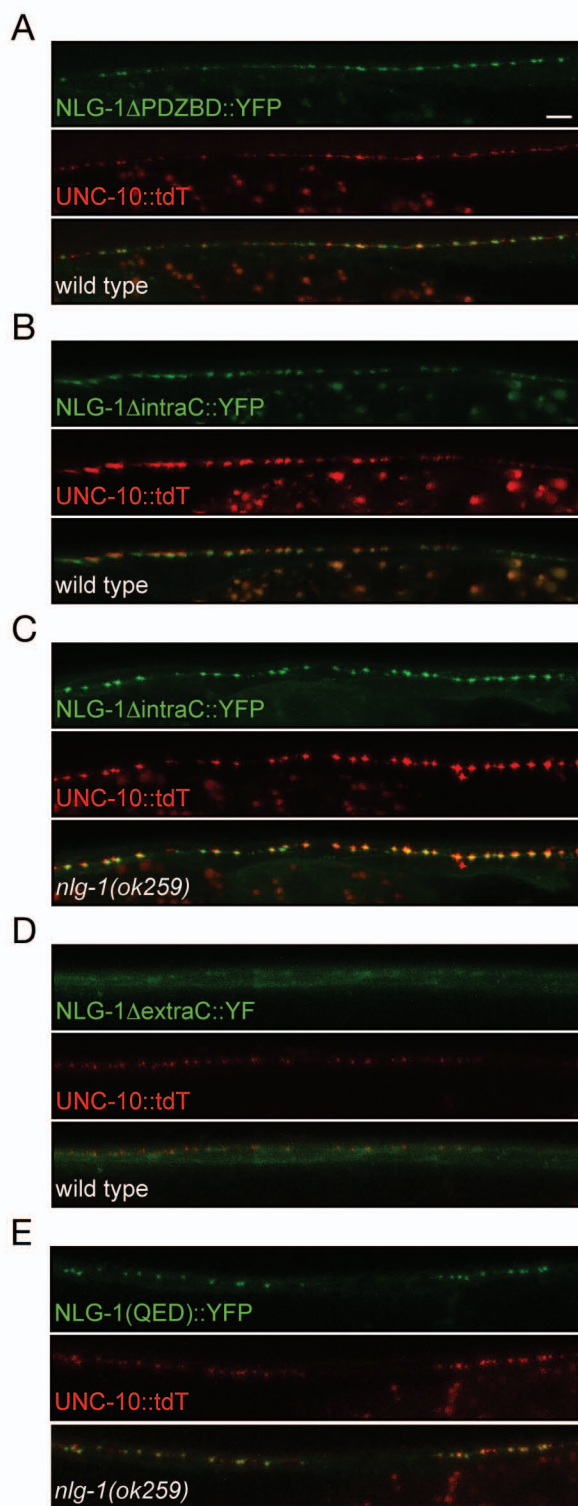


Figure S1, Related to Figure 3, NLG-1 clustering is independent of its intracellular tail, and relies on extracellular cues other than NRX-1

(A) An internally-tagged NLG-1 missing the C-terminal PDZ-binding domain (NLG-1 Δ PDZBD::YFP) localizes normally apposite to inhibitory presynaptic terminals. (B) The same construct lacking the entire cytoplasmic tail of NLG-1 (NLG-1 Δ intraC::YFP) also localizes to inhibitory postsynapses. (C) This is not due to dimerization with the endogenous NLG-1, since its distribution is unchanged in *nlg-1(ok259)* null mutants. (D) In contrast deletion of the extracellular domain of NLG-1 leads to a diffuse distribution of the corresponding protein (NLG-1 Δ extraC::YFP) at the cell plasma membrane. (E) A putative NRX-1 binding mutant of NLG-1, NLG-1(QED), shows a normal distribution at inhibitory postsynapses. (A—E) Inhibitory presynaptic terminals are visualized by expressing the active zone marker UNC-10::tdTomato under the control of the *unc-47* promoter. (F) Quantification of UNC-49::YFP clustering in wild-type, *nlg-1(ok259)* mutant and *nlg-1(ok259)* mutant animals expressing full-length or truncated NLG-1 constructs in body-wall muscles. The number of animals analyzed is indicated. $p < 0.001$, Fisher's exact test. p values are *** < 0.001 , **** < 0.0001 . Scale bar: 5 μ m.

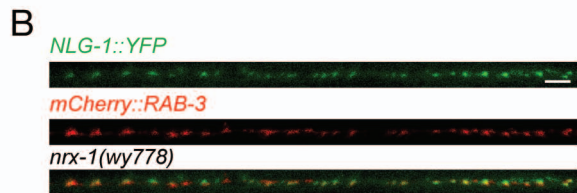
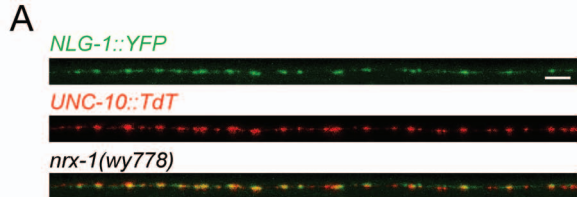


Figure S2, Related to Figure 3, Clustering of presynaptic active zones and synaptic vesicles is normal in *nrx-1* mutants

(A) The active zone protein UNC-10::TdT forms clusters apposite to NLG-1::YFP in *nrx-1(wy778)* animals. (B) Synaptic vesicles labeled with mCherry::RAB-3 accumulate normally at inhibitory presynaptic terminals in *nrx-1(wy778)* mutants.

Scale bar: 5 μ m.

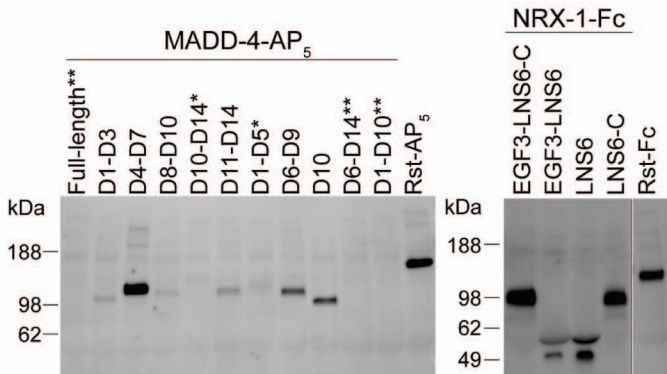


Figure S3, Related to Figure 6, Expression of MADD-4S and NRX-1 extracellular fragments in Drosophila S2 culture for the ECIA.

Double (**) and single (*) asterisks indicate no detectable expression and very low levels of expression, respectively.

